Supporting Information for

Latent Heat Flux Trend and Its Seasonal Dependence over the East China Sea Kuroshio Region

Chengji Chen[1,2], Qiang Wang[1,2]

[1]Key Laboratory of Marine Hazards Forecasting, Ministry of Natural Resources, Hohai University, Nanjing, China

[2]College of Oceanography, Hohai University, Nanjing, China

Contents of this file

Introduction

The Supporting Information accompanying this study serves as a complementary material to the main manuscript, aimed at providing a more comprehensive set of data and analyses to support the interpretation and inferences drawn from the primary findings.

Text S1. Mann-Kendall trend test

The Mann-Kendall trend test [45, 46] is a robust non-parametric method used to detect trends in time series data. It assesses the presence and direction of trends by comparing the ranks of data points within the series. The method does not require samples to adhere to specific distributions, and extreme values have no influence on the test results. Therefore, this method can determine whether a natural process exhibits a definite trend, making it suitable for trend analysis in oceanic and atmospheric studies.

Given a set of independent and randomly distributed time series $(x_1, x_2, \ldots, x_n)$, the test statistic is defined as follows:

$$S = \sum_{i=1}^{n-1} \sum_{j=i+1}^{n} sign(x_j - x_i), \quad (S1)$$

where n is the number of data points, x_j and x_i are data values at time points j and i respectively, $sign(\cdot)$ is the sign function which returns $+1$ for positive differences, -1 for negative differences, and 0 for ties. If $S > 0$, there is an increasing trend. If $S < 0$, there is a decreasing trend. If $S = 0$, there is no trend.

To determine significance, the Z-statistic is typically employed, calculated as:

$$Z = \frac{S - \mu_S}{\sigma_S}, \quad (S1)$$

where μ_S is the excepted values of S, which is 0. The σ_S is the standard deviation of S, calculated as:

$$\sigma_S^2 = \frac{n(n-1)(2n+5) - \sum_{p-1}^{g} t_p(t_p - 1)(2t_p + 5)}{18}, \quad (S3)$$

here, g represents the number of groups of tied ranks, and t_p denoted the number of tied ranks within the pth group.

Then, the significance of S can be determined based on the value of the Z-statistic. Typically, S is considered significant when $|Z| \geq Z_{\alpha/2}$, where $Z_{\alpha/2}$ is the critical value corresponding to a significance level α. For a 95% significance level, the critical value $Z_{\alpha/2}$ is 1.96. For a 99% significance level, the critical value $Z_{\alpha/2}$ is 2.576.

Text S2. NOAA-CIRES-DOE 20th Century Reanalysis V3 (20CRv3)

The 20CRv3 is the latest version of 20CR project data production. The 20CRv3 system employs an 80-member ensemble Kalman filter to assimilate sea surface observations exclusively from the freely accessible International Surface Pressure Databank (ISPD) version 4.7 [50, 51]. These observations are assimilated into the U.S. National Centers for Environmental Prediction (NCEP) Global Forecast System (GFS) model, version 14.0.1. The GFS model features a spectral horizontal resolution of T254

(i.e. 60 km at the equator) and a vertical atmospheric resolution with 64 levels up to approximately 0.3 hPa. Sea surface temperature (SST) fields are prescribed from two eight-member ensembles: version 3 of the Simple Ocean Data Assimilation with sparse input for the period 1836–1980 [52], and the Hadley Centre Sea Ice and SST dataset, version 2.2 (HadISST2.2), for the period 1981–2015. These SST fields, originally available as 5-day averages, are interpolated to daily resolution for 20CRv3. Sea ice concentration fields are prescribed from monthly HadISST2.3 [53], which has been interpolated to daily resolution. Solar radiation is calculated based on the Total Solar Irradiance (TSI) Reconstruction derived from the Naval Research Laboratory TSI (NRLTSI2 [54]). Additionally, time-varying atmospheric constituents, including volcanic aerosols [55], stratospheric ozone [56], and atmospheric carbon dioxide (CO2) levels [57], are specified in the model. The output provides subsurface land fields, such as soil moisture, as well as surface and atmospheric fields at 3-hourly intervals. This dataset is available at https://www.psl.noaa.gov/data/gridded/data.20thC_ReanV3. We use 20CRv3 monthly 1°× 1° gridded ensemble mean LHF data from 1959 to 2015.

Text S3. Objectively Analyzed Air-Sea Fluxes (OAFlux)

The OAFlux project supplies heat flux data for global ice-free ocean basins. These heat flux values are calculated using the COARE 3.0 bulk flux algorithm based on the combination of satellite data and information from three atmospheric reanalysis sources: NCEP1, NCEP2, and ERA-40 [40]. The satellite-derived wind speed data is from three instruments: the Special Sensor Microwave Imager (SSMI), the Advanced Microwave Scanning Radiometer for Earth Observing System (AMSR-E), and QuikSCAT. Near-surface humidity is determined from SSMI column water vapor retrievals [58] and adjusted to a 2-meter height using the COARE 3.0 algorithm. SST data are obtained from NOAA's optimum interpolation method [59]. We utilize the third version of the OAFlux dataset, which covers a period of 38 years (1985–2022) with daily temporal resolution and a grid resolution of 1°. This dataset is available at http://apdrc.soest.hawaii.edu/datadoc/whoi_oafluxday. We use OAFlux daily gridded LHF data from 1986 to 2021 to estimate LHF trends over the ECSKR.

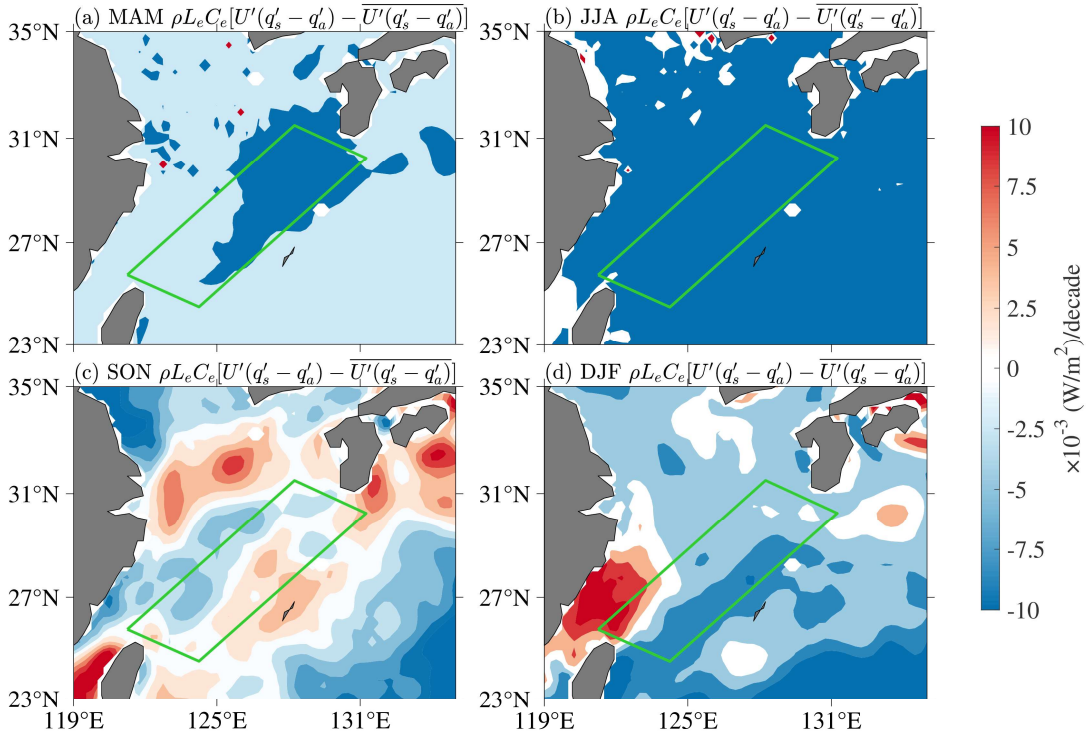

Figure S1. Slope distribution of 11-years running mean monthly $\rho_a L_e C_e\left[U'(q_s' - q_a') - \overline{U'(q_s' - q_a')}\right]$ trend components for four seasons during 1959–2021.

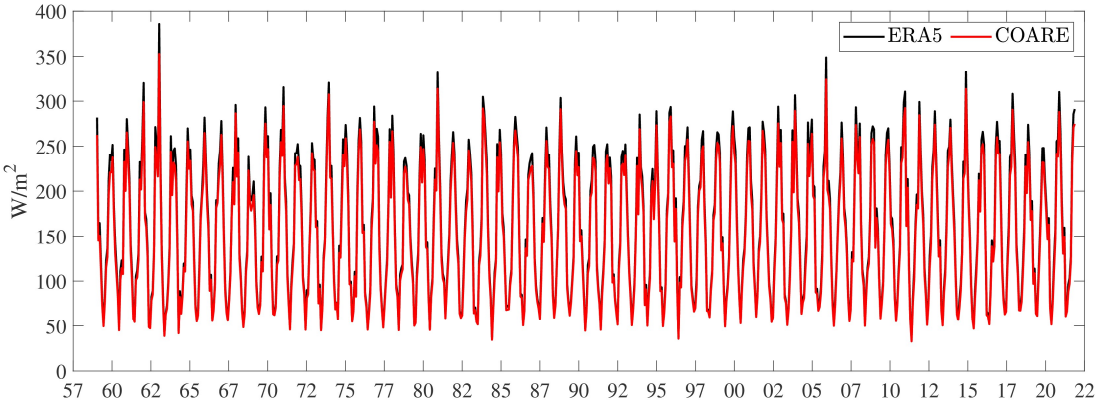

Figure S2. Time series of LHF by ERA5 (black line) and COARE (red line) algorithm from 1959 to 2021 over the ECSKR.

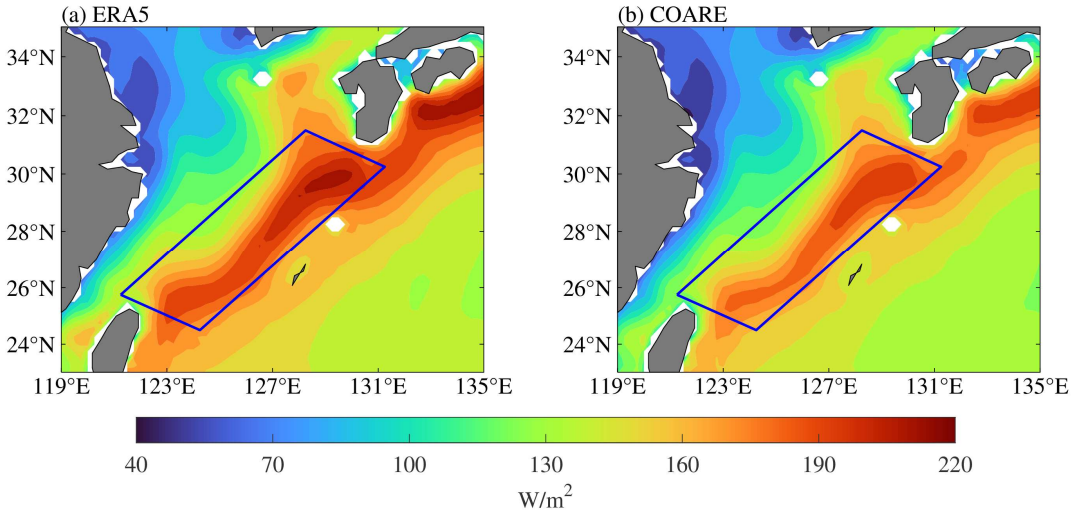

Figure S3. Climatology LHF by (a) ERA5 and (b) COARE algorithm.

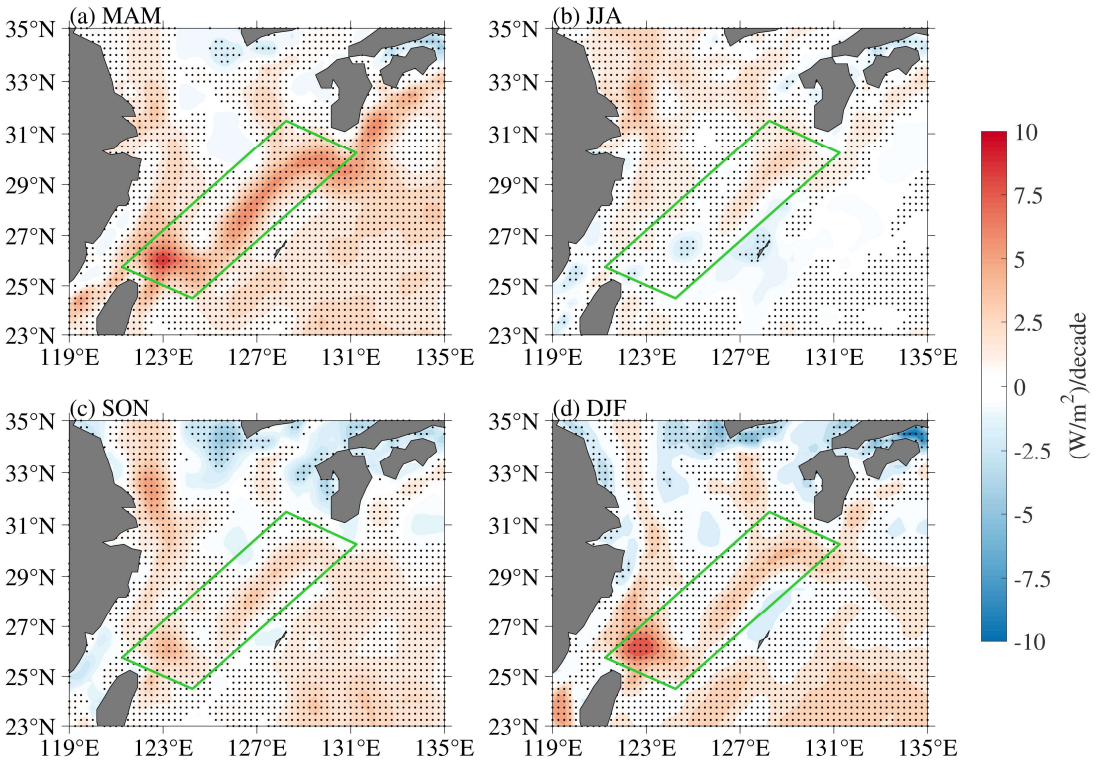

Figure S4. The linear trends of LHF in (a) spring, (b) summer, (c) fall and (d) winter. The dotted regions indicate that the trend of LHF passes the Mann-Kendall trend test at the 95% significance level.

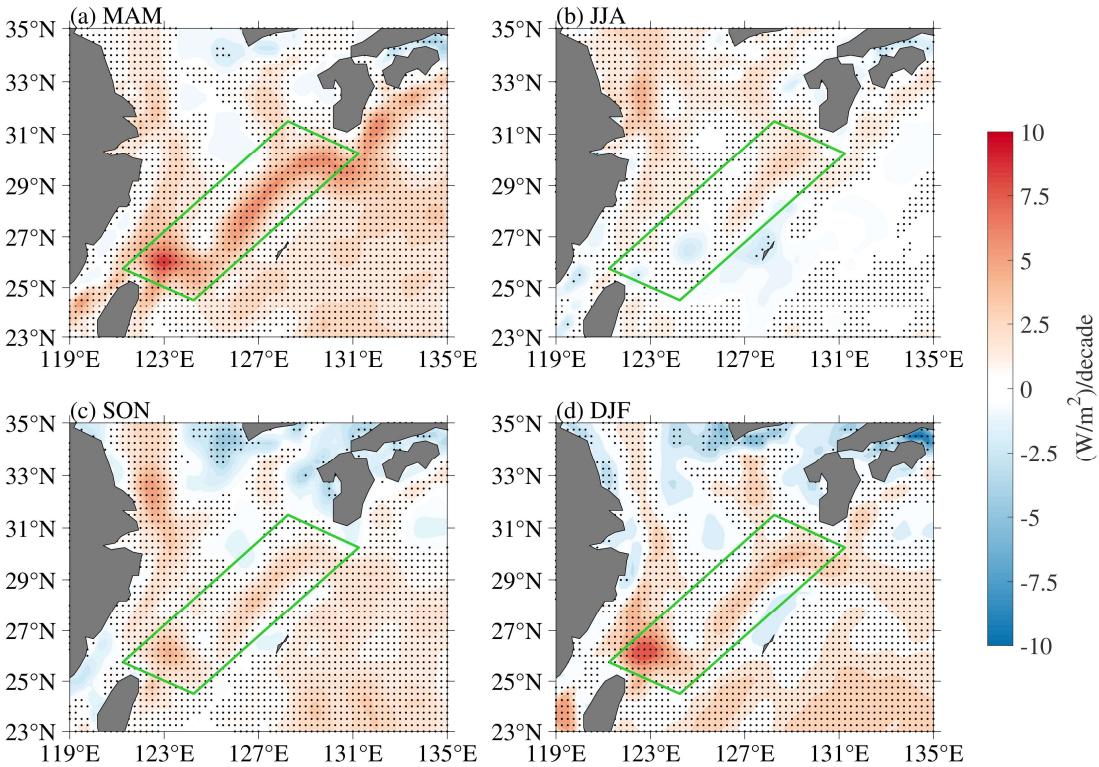

Figure S5. Same as Figure S3, but the dotted regions indicate that the trend of LHF passes the Mann-Kendall trend test at the 99% significance level.

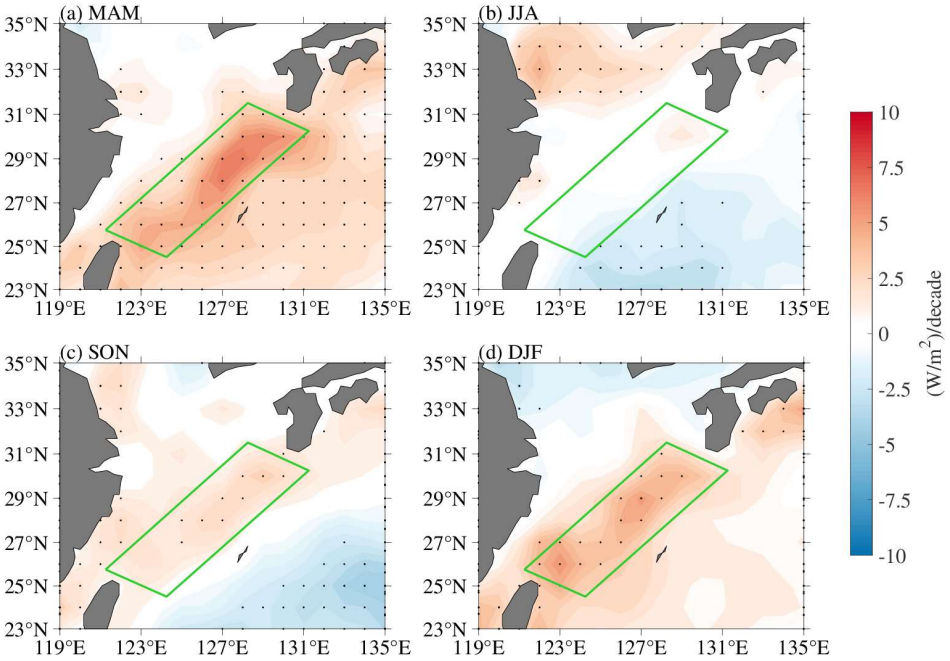

Figure S6. LHF trends in (a) spring, (b) summer, (c) fall and (d) winter over ECSKR using 20CRv3 from 1959 to 2015. The green box is located on the Kuroshio current axis. The dots indicate the confidence level exceeding 95% based on Student's *t*-test.

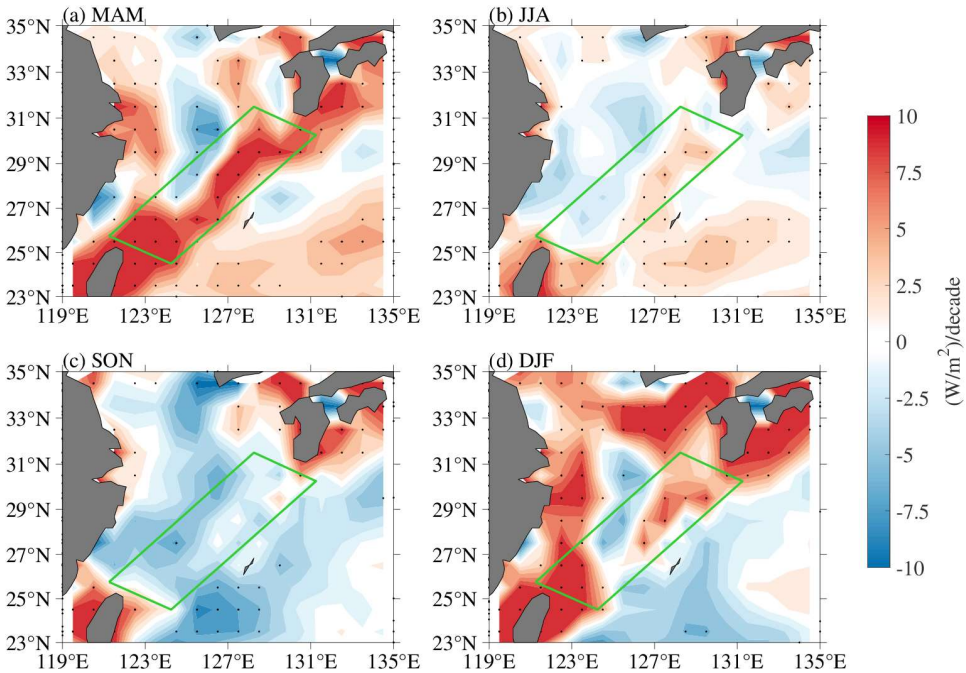

Figure S7. Same as Figure S5, but for OAFlux from 1986 to 2021.

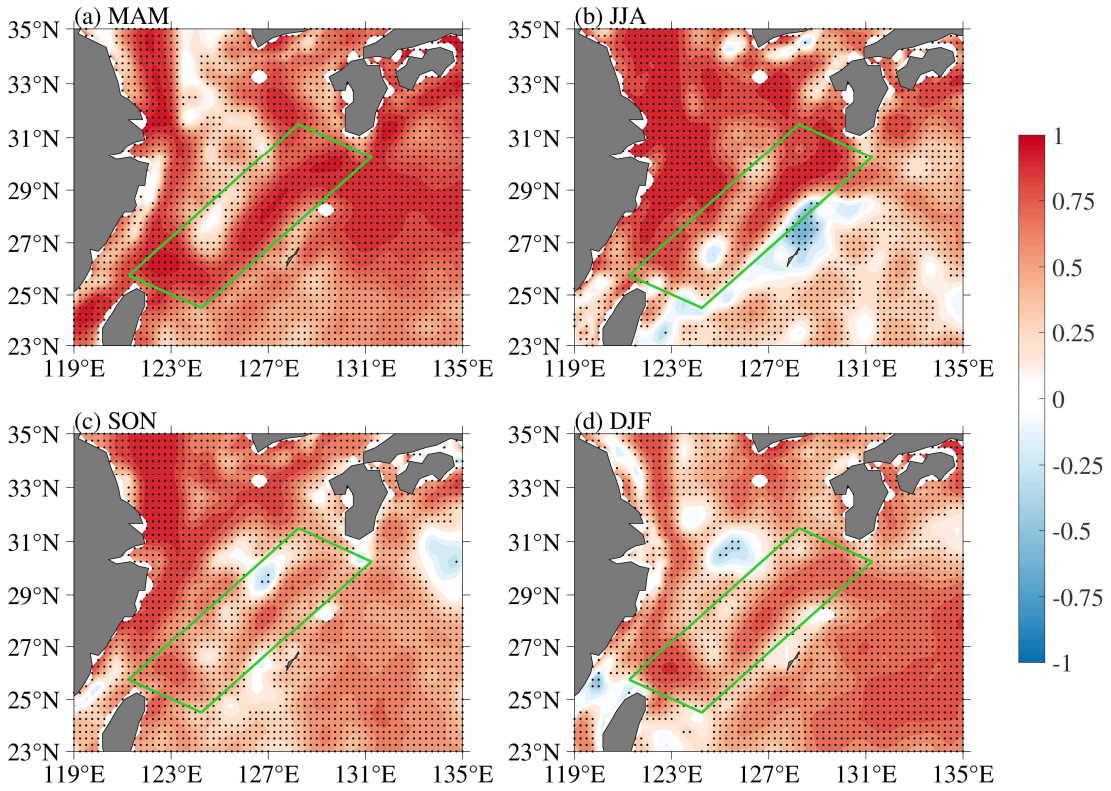

Figure S8. Spatial distribution of correlation between LHF and SST. All variables are conducted with a 11-year running mean. Dotted area indicates the correlation coefficient passing 95% significant level test.